Journal of Magnetism and Magnetic Materials 321 (2009) 1714–1718

Contents lists available at ScienceDirect

Journal of Magnetism and Magnetic Materials

journal homepage: www.elsevier.com/locate/jmmm

Local structure of multiferroic RMn_2O_5: Important role of the R site

T.A. Tyson [a,c,*], Z. Chen [a], M.A. DeLeon [a], S. Yoong [b,c], S.-W. Cheong [b,c]

[a] Department of Physics, New Jersey Institute of Technology, Newark, NJ 07102, USA
[b] Department of Physics and Astronomy, Rutgers University, Piscataway, NJ 08854, USA
[c] Rutgers Center for Emergent Materials, Rutgers University, Piscataway, NJ 08854, USA

ARTICLE INFO

Available online 11 February 2009

PACS:
77.80.−e
78.70.Dm
64.70.Kb

Keywords:
XAFS
Multiferroic
Local structure

ABSTRACT

The temperature and magnetic field dependent local structure of RMn_2O_5 systems was examined. While no significant displacements of the Mn ions are observed, it is found that the R–O distribution exhibits changes at low temperature which are possibly related to the changes in the electric polarization. Density functional computations are used to explore the system dynamics and to link the local structural measurements with anomalous changes in the infrared absorption spectra. The anomalous R–O distribution and observed coupling to magnetic fields point to the need to properly treat the 4f electrons on the R sites in these systems.

1. Introduction

Magnetic and ferroelectric materials have been extensively studied for several decades from both applied and basic research perspectives. This work has resulted in the development of devices ranging from transformers to hard drive read–head sensors and data storage media [1–3]. Reductions in size and enhancement of sensitivity of magnetic devices, for example, have led to the large increases in data storage capacity with time.

From a microscopic perspective, magnetization can occur as a result of alignment of equivalent spins (ferromagnetism) or antialignment of non-equivalent spins (ferrimagnetism). Non-collinear alignment/antialignment of spins can also produce a net magnetization called canted ferromagnetism/antiferromagnetism. In these materials, the spontaneous magnetization (magnetic polarization) can be reversed and cycled.

For ferroelectric systems, the simple perovskite ABO_3 systems such as ($PbTiO_3$) have been extensively studied [2]. These materials possess a spontaneous net polarization below the so-called ferroelectric transition temperature and exhibit analogous hysteresis in the presence of an externally applied electric filed. From a microscopic perspective these materials can acquire a net electric polarization due to atomic displacement such as in the ABO_3 system where an off center B atom displacement is proposed.

In the ideal displacive ferroelectric system, a symmetry reduction occurs on entering the ferroelectric phase from the high-temperature paraelectric phase. Typical atomic off-center displacements of Ti and Pb in $PbTiO_3$ are approximately 0.2 Å (from XAFS) with onset 190 K above T_c [4]. XAFS analysis has become an invaluable tool for studying ferroelectrics as can be seen from studies on $KTa_{0.91}Nb_{0.09}O_3$ [5(a)], $KNbO_3$ [5(b)], $BaTiO_3$[5(c)], $PbZr_{1-x}Ti_xO_3$ [5(d)], $BaTi_{1-x}Zr_xO_3$ [5(e)].

Magneto-electric multiferroics are a class of materials which are simultaneously ferroelectric and ferromagnetic [3,6]. The possibility of coupling of the magnetic and electric properties will enable new functions. These include the ability to store data as both magnetic and electrical bits and the ability to write ferroelectric bits with magnetic fields. Although broad classes of ferromagnetic materials and ferroelectric materials exist, not many multiferroelectric systems have been observed. It has been suggested in by Hill [3] that while the 3d occupancy on ABO_3 systems creates unpaired electrons needed for magnetism it also stabilizes inversion center preserving distortions. Magneto-electric effects have been explored in systems such as Ti_2O_3, $GaFeO_3$, boracite, $TbPO_4$, $BiFeO_3$ and $BiMnO_3$ [6] The characteristic feature of these systems is the weak coupling between the magnetic and electric components.

Hur et al. [7] discovered reversible switching below 40 K in the system $TbMn_2O_5$ (composed of *c*-axis MnO_6 polyhedral chains cross-linked by MnO_5 pyramids, Fig. 1). By sweeping the magnetic field from zero to two Tesla the polarization passes through zero and attains a value with magnitude ~equal to the zero field value. Reducing the field to zero recovers the initial state. The magnitude of the polarization in zero field is ~40 nC/cm^2. Thus the RMn_2O_5 system shows promise for enabling an understanding of the

* Corresponding author at: Department of Physics, New Jersey Institute of Technology, Newark, NJ 07102, USA. Tel.: +1 973 642 4681; fax: +1 973 596 5794.
E-mail address: tyson@ADM.NJIT.EDU (T.A. Tyson).

0304-8853/$ - see front matter © 2009 Elsevier B.V. All rights reserved.
doi:10.1016/j.jmmm.2009.02.017

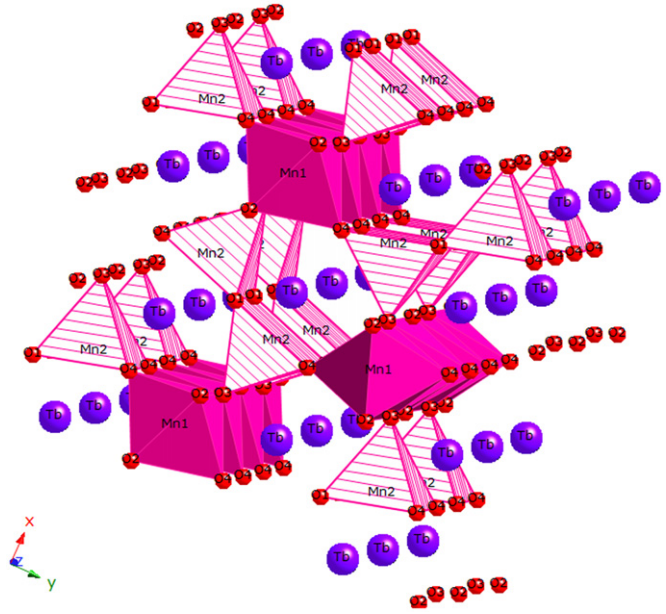

Fig. 1. Crystal structure of $TbMn_2O_5$ showing the corner sharing $Mn1O_6$ polyhedra linked along the *z*-axis. Note the cross linked Mn_2O_5 pyramids.

coupling spin and lattice degrees of freedom and for the development of devices (if the magnetic and electrical transition temperatures can be increased and the sensitivity to magnetic fields is enhanced.)

The room temperature structure of RMn_2O_5 for a broad range of R ions have has been determined [8]. The $Mn^{4+}O_6$ octahedra (Mn1 sites) form infinite chains parallel to the *c*-axis of the orthorhombic Pbam cell (Fig. 1). These chains are cross-linked by $Mn^{4+}O_5$ pyramids (Mn2 sites) which form edge-sharing dimmers ($Mn_2^{4+}O_8$). The R atoms are eight-fold coordinated to oxygen atoms. We note that the inversion center in this Pbam space group is inconsistent with a finite polarization. The low-temperature behavior of this system is quite complex [9]. The Mn sites order antiferromagnetically at T_N ~40 K (43 for Tb and 44 K for Dy) followed by the onset of ferroelectricity at 38 K for Tb (and 39 K for Dy). For the Tb system, the magnetic structure is incommensurate directly below T_N and becomes commensurate on cooling through a "lock-in" temperature at 33 K. A commensurate to incommensurate transition takes place at 24 K concomitant with a reduction in **|P|** (magnitude of polarization**).** Ordering of the Tb moments onsets near 9 K with recovery of **|P|**. For the case of Dy, the magnetic structure is incommensurate below 32 K and the magnetic structure is maintained until 8 K at which the Dy moments order and a commensurate spin order is observed.

In this system it is suggested that the inhomogeneous magnetization due locally to spin frustration enables the observed low-temperature coupling of magnetization and polarization. A view about the Tb *c*-axis chains (Fig. 1) reveals that the Mn ions are arranged as rings of Mn^{4+}–Mn^{3+}–Mn^{4+}–Mn^{3+}–Mn^{3+} ions with $S=2$ and $S=\frac{3}{2}$ for the Mn^{4+} and Mn^{3+} ion, respectively [10]. The nearest neighboring spins are antiferromagnetically coupled but due to the odd number of spins on the loops all AF couplings cannot be achieved leading to magnetic frustration. This produces a large number of magnetic configurations with closely lying energies. Across the loop, half of the Mn^{3-} Mn^{4+} ions spins are parallel and the other half are coupled in a antiparallel manner. It is argued that the total energy can be lowered by breaking the symmetry by displacement (small) of the Mn^{3+} ions towards or away for the apical oxygen ions resulting in a net polarization along the *b*-axis at low temperatures.

Although earlier neutron scattering measurements suggest a lower symmetry than the standard Pbam space group [11], no recent evidence has been found structurally for a reduction in the space group symmetry by diffraction measurements at room temperature. X-ray diffraction measurements reveal suprelattice reflections in $DyMn_2O_5$ in the low temperature magnetically ordered regions [12] No significant field or temperature-dependent changes in the lattice parameters have been found in the RMn_2O_5 system by high resolution diffraction methods [13].

In order to understand the mechanism responsible for the finite polarization from a microscopic perspective, temperature and magnetic field dependent local structural measurements have been performed. To the limit of the experiments (0.01 Å) no displacement of the Mn ion was detected on comparing low- and high-temperature measurements or measurements in magnetic fields. However, temperature and magnetic field changes were found in the R–O distributions. This suggests that the R site plays an important role in the magnetic and electrical properties of these materials.

2. Experimental and theoretical methods

Polycrystalline samples of $TbMn_2O_5$ and $DyMn_2O_5$ were prepared by solid state reaction in oxygen. X-ray absorption samples were prepared by grinding and sieving the materials (500 mesh) and brushing them onto Kapton tape. Layers of tape were stacked to produce a uniform sample for transmission measurements with jump $\mu t \sim 1$. Spectra were measured at NSLS beamline X19A at Brookhaven National Laboratory. Measurements were made on warming from 3 K in He vapor in the cryostat of a superconducting magnet [14]. Magnetic field measurements were conducted at 3 K. The reduction of the X-ray absorption fine-structure (XAFS) data was performed using standard procedures and follows the details of Ref. [15].

Local spin density functional calculations in the projector augment wave approach [16] were carried out using a 32 atom cell. Full optimization of both the lattice parameters and atomic positions was conducted and the GGA+U approximation was implemented to obtain the fully relaxed structure. The structure was optimized so that forces on each atom were below 3×10^{-5} eV/Å. Forces along *x*-, *y*- and *z*-direction were computed for all 32 atoms for displacements of 0.002 (fraction coordinates). Forces for positive and negative displacements were averaged to improve the accuracy. The phonons at gamma point in the Brillouin zone were determined by frozen phonon lattice dynamics calculations [17,18].

3. Results and discussion

We combine previous temperature-dependent data on the Tb system [15] with recent field-dependent data on the Dy system. In Fig. 2(a), we show the Fourier transform of the Tb L3 spectra taken at 20 K (thin line) and 300 K (thick line). These spectra are compared with a model spectrum, based on the Pbam structure [10(b)] including a reasonable global Debye–Waller factor (same for all shells) of $\sigma^2=0.0023$ Å^2 for low temperature (dotted line). The Tb–Mn and higher shells (Tb–Tb and Tb–Mn shells) are matched by this simple model. However, the Tb–O shell (shown in Fig. 2(a)) exhibits a significant deviation from the diffraction derived model. The low-temperature (thin line) data reveal a broad, suppressed and asymmetric function compared to the model suggesting a complex distribution. The filtered first shell XAFS spectrum (Fig. 2(b)) reveals a "beat" pattern corresponding to multiple components leading to a reduction in amplitude at

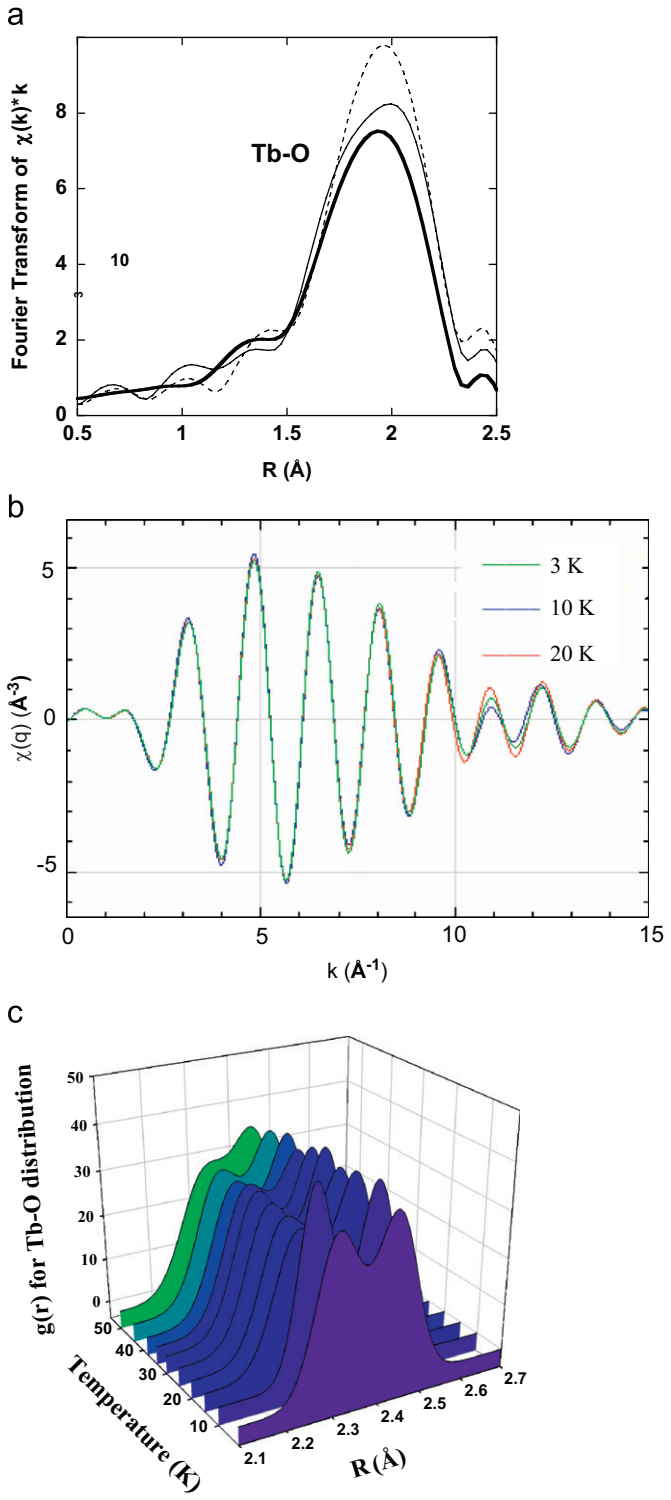

Fig. 2. Temperature-dependent XAFS Fourier transform of the Tb–O shell (a), the filtered fine-structure (b) and the radial distribution function (c) In (b) note the "beat" in the spectra near 11 $Å^{-1}$ indicating the splitting of the Tb–O shell.

approximately 11 $Å^{-1}$. The position of the "beat" pattern yields a splitting of ~0.14 Å. The split radial distribution derived from direct fits is given in Fig. 2(c). Detailed multiple shell analysis was conducted for the Tb–O distribution [15]. Below ~180 K the Tb–O distribution is composed of well-resolved components which sharpen in intensity at the Tb ordering temperature.

A structure which preserves the local atomic order with respect to the Mn polyhedra and the second shell about Tb (Tb–Mn and higher shells) while hosting a split Tb–O distribution has limited possibilities. The data are consistent with rotations of the polyhedra about the *c*-axis generated by bucking at the "hinges" connecting them [15].

The self-force constants [19], which indicate the force on the isolated atom with respect to unit displacements, are all positive indicating that the optimized structure is stable with respect to the displacement of individual atoms. No "ratting" atoms are present in the structure. All atoms sit in single position wells. The total energy can only be lowered by the cooperative motion of different atoms.

The atomic structure is found to be sensitive to the magnetic ordering and points to the need to incorporate a proper treatment of the 4f electrons as localized valence states (not core states) with correlation treated appropriately.

While the Mn1 ions reside in approximately symmetric potential wells with approximately equal force constants for *x*, *y* and *z* displacements (k_x, k_y, $k\_z = \sim 25, 26, 30$ eV/$Å^2$), the Mn2 ions have force constants of ~23 eV/$Å^2$ in the *y*–*z* plane and ~12 eV/$Å^2$ along the *x*-axis. The O1 (k_x, k_y, $k\_z = \sim 25, \sim 26,$

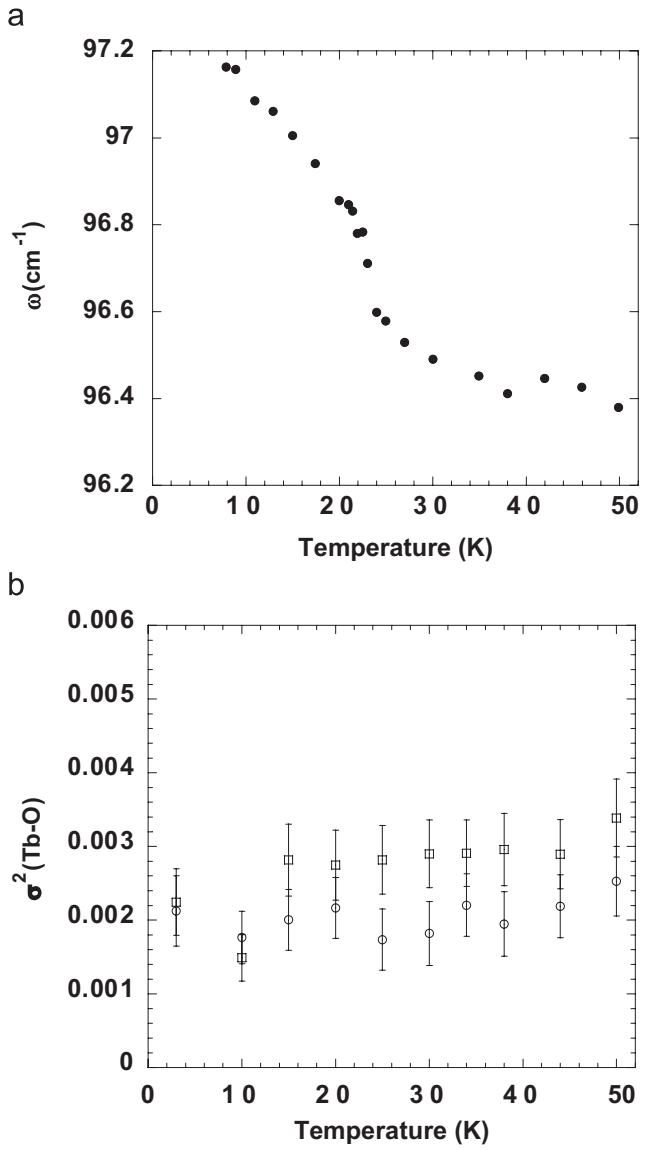

Fig. 3. Anomalous low-temperature hardening of 97 cm^{-1} phonon (Aguilar et al. [20]). The hardening coincides with the width of the Tb–O components becoming more equivalent on cooling.

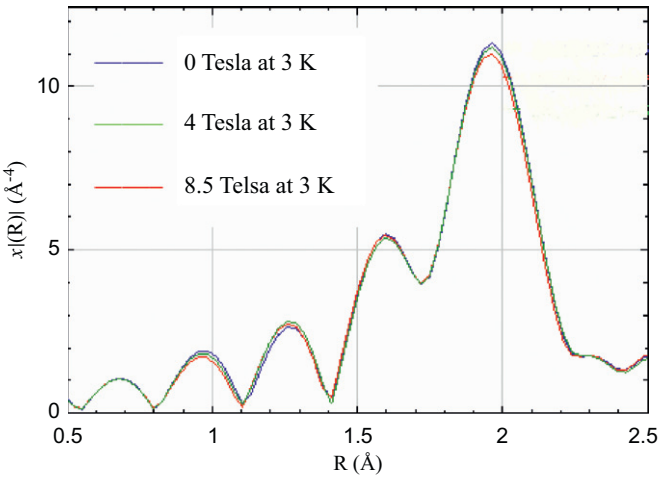

Fig. 4. Fourier transform of Dy L3 spectrum showing the Dy–O distribution for data taken at 3 K with magnetic fields strengths of 0 (blue), 4 (green) and 8.5 T (red). Note the suppression of the main peak amplitude with increased magnetic field. The statistical uncertainty is approximately equal to the line thickness. (For interpretation of the references to colour in this figure legend, the reader is referred to the web version of this article.)

~30 eV/Å^2), O3 (~17, ~7, ~14 eV/Å^2) and O4 (~8, 16, 13 eV/Å^2) ions also exhibit asymmetric potential wells. The corresponding parameters for Tb are ~11, ~14, ~10 eV/Å^2. (The O2 sites have highly symmertric potentials with $k\_x \sim k\_y \sim k\_z \sim 12$ eV/Å^2.)

The low-energy phonons ~near 100 cm^{-1} were computed from the dynamic matrix. Analysis of the eigenvectors reveals that strong coupling of the Tb and O sites is involved in these modes and not purely Tb displacements. This enables one to link the observed XAFS measurement with anomalies found in optical measurements.

In optical measurements the frequency of the low-energy phonon was found to increase anomalously at low temperature (Fig. 3(a)) [20]. The hardening of the phonons can be compared with the gain in symmetry for the two components in the Tb–O distribution as temperature is lowered. The split peaks σ^2 parameters become more equivalent at low temperature and suggests a connection with the optical measurements.

The importance of the R–O distribution can again be seen more directly in magnetic field dependent measurements on $DyMn_2O_5$. At low temperatures, this system is known to have a strong dependence of the dielectric constant and electric polarization on magnetic fields [21]. Measurement of the variation of the amplitude of the XAFS structure function (Fig. 4) for the Dy–O distribution with magnetic field reveals that the amplitude decreases with increased field. No changes in the Mn–O distribution are found (within the experimental errors). As in the case of the Tb system (temperature-dependent changes) the field-dependent changes, in the simplest model, are associated with rotation of the MnO_6 polyhedra which can possibly break the Pbam symmetry.

4. Summary

The observed temperature and field-dependent changes which dominate in the R–O distribution suggest that the origin of a finite polarization in RMn_2O_5 system is connected, in part, with rotation of the MnO_X polyhedra which lower the symmetry from Pbam. This system is possibly an improper ferroelectric analogous to the hexagonal system $YMnO_3$ where tilting of the Mn centered polyhedra yields a large polarization due to buckling of the Y–O layers without significant off-center shifts of the Mn ions [22]. For R sites with 4f electrons, the observations point to the need to properly treat the 4f electron states since the magnetic states on the R sites are coupled with the atomic structure.

Acknowledgments

This work is supported by DOE Grants DE-FG02-07ER46402 and DE-FG02-07ER46382. This research used resources of the National Energy Research Scientific Computing Center, which is supported by the Office of Science of the US DOE under Contract no. DE-AC02-05CH11231.

References

[1] [a] R.C. O'Handley, Modern Magnetic Materials, Wiley, New York, 2000;
[b] S.X. Wang, A.M. Taratorin, Magnetic Information Storage Technology, Academic Press, San Diego, 1999;
[c] Peter Grunberg, Phys. Today (2001);
[d] W.E. Pickett, J.S. Moodera, Phys. Today (2001);
[e] Special Issue Magnetoelectronics, Physics Today April 1995.
[2] [a] M. Okuyama, Y. Ishibashi, Ferroelectric Thin Films: Basic Properties and Device Physics for Memory Applications, Springer, Berlin, 2005;
[b] M. Dawber, K.M. Rabe, J.F. Scott, Rev. Mod. Phys. 77 (2005) 1083;
[c] N.A. Spaldin, Science 304 (2004) 1606;
[d] T.M. Shaw, S. Trolier-McKinstry, P.C. McIntyre, Annu. Rev. Mater. Sci. 30 (2000) 263;
[e] Y. Girshberg, Y. Yacoby, Solid State Comm. 103 (1997) 425;
[f] M.T. Dove, Am. Mineral. 82 (1997) 213;
[g] M.E. Lines, A.M. Glass, Principles and Applications of Ferroelectrics and Related Materials, Calderon, Oxford, 1977.
[3] N.A. Hill, J. Phys. Chem. 104 (2000) 6694.
[4] N. Sicron, B. Ravel, Y. Yacoby, E.A. Stern, F. Dogan, J.J. Rehr, Phys. Rev. B 50 (1994) 13168.
[5] [a] O. Hanske-Petitpierre, Y. Yacoby, J. Mustre de Leon, E.A. Stern, J.J. Rehr, Phys. Rev. B 44 (1991) 6700;
[b] A.I. Frenkel, F.M. Wang, S. Kelly, R. Ingalls, D. Haskel, E.A. Stern, Y. Yacoby, Phys. Rev. B 56 (1997) 10869;
[c] B. Ravel, E.A. Stern, R.I. Vedrinskii, V. Kraizman, Ferroelectrics 206 (1998) 407;
[d] D. Cao, I.-K. Jeong, R.H. Heffner, T. Darling, J.-K. Lee, F. Bridges, J.-S. Park, K.-S. Hong, Phys. Rev. B 70 (2004) 224102;
[e] C. Laulhé, F. Hippert, J. Kreisel, M. Maglione, A. Simon, J.L. Hazemann, V. Nassif, Phys. Rev. B 74 (2006) 014106.
[6] [a] M. Fiebig, J. Phys. D 38 (2005) R123;
[b] N. Spalding, M. Fiebig, Science 309 (2005) 391;
[c] W. Prellier, M. Singh, P. Murugavel, J. Phys. Condens. Matter 17 (2005) R803.
[7] N. Hur, S. Park, P.A. Sharma, J.S. Ahn, S. Guha, S.-W. Cheong, Nature 429 (2004) 392.
[8] [a] S.C. Abrahams, J.L. Bernstein, J. Chem. Phys. 46 (1967) 3776;
[b] J.A. Alonso, M.T. Casais, M.J. Martinez-Lope, J.L. Martinez, M.T. Fernandez-Diaz, J. Phys.: Condens. Matter 9 (1997) 8515;
[c] J.A. Alonso, M.T. Casais, M.J. Martinez-Lope, I. Rasines, J. Solid State Chem. 129 (1997) 105;
[d] G. Popov, M. Greenblatt, W.H. McCarroll, B Mater. Res. Bull. 35 (2000) 1661 (and references therein);
[e] I. Kagomiya, K. Kohn, T. Uchiyama, Ferroelectrics 280 (2002) 131;
[f] A. Munoz, J.A. Alonso, M.T. Casais, M.J. Martinez-Lope, J.L. Martinez, M.T. Fernandez-Diaz, Phys. Rev. B 65 (2002) 144423;
[g] A. Munoz, J.A. Alonso, M.T. Casais, M.J. Mairtinez-Lope, J.L. Martinez, M.T. Fernandez-Diaz, Eur. J. Inorg. Chem. Phys. Rev. B 4 (2005) 685.
[9] [a] L.C. Chapon, G.R. Blake, M.J. Gutmann, S. Park, N. Hur, P.G. Radaelli, S.W. Cheong, Phys. Rev. Lett. 93 (2004) 177402/1;
[b] G.R. Blake, L.C. Chapon, P.G. Radaelli, S. Park, N. Hur, S.-W. Cheong, J. Rodríguez-Carvajal, Phys. Rev. B 71 (2005) 214402.
[10] S.W. Cheong, M. Mostoyov, Nat. Mater. 6 (2007) 13 (and references therein).
[11] V. Polyak, V. Plakhty, M. Bonnet, P. Burlet, L. -P. Regnault, S. Gavrilov, I. Zobkalo, O. Smirnov, Phys. B: Condens. Matter 297 (2001) 208.
[12] D. Higashiyama, S. Miyasaka, N. Kida, T. Arima, Y. Tokura, Phys. Rev. B 70 (2004) 174405.
[13] I. Kagomiya, S. Matsumoto, K. Kohn, Y. Fukuda, T. Shoubu, H. Kimura, Y. Noda, N. Ikeda, Ferroelectrics 286 (2002) 167.
[14] [a] see www site 〈http://eies.njit.edu/~tyson/Supmagnet.html〉;
[b] T.A. Tyson, M. Deleon, M. Croft, V.G. Harris, C.C. Kao, J. Kirkland, S.W. Cheong, Phys. Rev. B 70 (2004) 024410/1.
[15] T.A. Tyson, M. Deleon, S. Yoong, S.W. Cheong, Phys. Rev. B: Condens. Matter Mater. Phys. 75 (2007) 174413/1.
[16] G. Kresse, D. Joubert, Phys. Rev. B 59 (1999) 1758.
[17] K. Parlinski, Z.Q. Li, Y. Kawazoe, Phys. Rev. Lett. 78 (1997) 4063.

[18] Eigenvectors and eigenvalues of the dynamical matrix were computed by FROPHO (〈http://fropho.sourceforge.net/〉).
[19] P.h. Ghosez, E. Cockayne, U.V. Wagjmare, K. Rabe, Phys. Rev. B 60 (1999) 836.
[20] R. Valdes Aguilar, A.B. Sushkov, S. Park, S.-W. Cheong, H.D. Drew, Phys. Rev. B 74 (2006) 184404.
[21] N. Hur, S. Park, P.S. Sharma, S. Guha, S.-W. Cheong, Phys. Rev. Lett. 93 (2004) 107207.
[22] [a] B.B. Van Aken, T.T.M. Palstra, A. Filippetti, N.A. Spaldin, Nat. Mater. 3 (2004) 164;
[b] C.J. Fennie, K.M. Rabe, Phys. Rev. B. 72 (2005) 100103.